

# Indole-3-carbinol (I3C) increases apoptosis, represses growth of cancer cells, and enhances adenovirus-mediated oncolysis

Lan Chen<sup>1</sup>, Pei-Hsin Cheng<sup>2</sup>, Xiao-Mei Rao<sup>3</sup>, Kelly M McMasters<sup>1,2,3</sup>, and Heshan Sam Zhou<sup>1,3,4,\*</sup>

<sup>1</sup>Department of Surgery; University of Louisville School of Medicine; Louisville, KY USA; <sup>2</sup>Department of Pharmacology and Toxicology; University of Louisville School of Medicine; Louisville, KY USA; <sup>3</sup>James Graham Brown Cancer Center; University of Louisville School of Medicine; Louisville, KY USA;

<sup>4</sup>Department of Microbiology and Immunology; University of Louisville School of Medicine; Louisville, KY USA

**Keywords:** I3C, adenovirus, virotherapy, cyclin E, cancer prevention, oncolysis, cancer

**Abbreviations:** I3C, Indole-3-carbinol; Ad, adenovirus; WT, wild type; MOI, multiplicity of infection; CPE, cytopathic effect

Epidemiological studies suggest that high intake of cruciferous vegetables is associated with a lower risk of cancer. Experiments have shown that indole-3-carbinol (I3C), a naturally occurring compound derived from cruciferous vegetables, exhibits potent anticarcinogenic properties in a wide range of cancers. In this study, we showed that higher doses of I3C ( $\geq 400 \mu\text{M}$ ) induced apoptotic cancer cell death and lower doses of I3C ( $\leq 200 \mu\text{M}$ ) repressed cancer cell growth concurrently with suppressed expression of cyclin E and its partner CDK2. Notably, we found that pretreatment with low doses of I3C enhanced Ad-mediated oncolysis and cytotoxicity of human carcinoma cells by synergistic upregulation of apoptosis. Thus, the vegetable compound I3C as a dietary supplement may benefit cancer prevention and improve Ad oncolytic therapies.

## Introduction

Human adenoviruses (Ads) are double-stranded linear DNA viruses that are able to infect and replicate in a wide variety of cell types. The viral genome is divided into early and late genes relative to the onset of viral DNA replication. The Ad *E1* region contains two sets of genes, *E1a* and *E1b*, that are dedicated to cell cycle control, apoptotic inhibition, and cellular and viral gene regulation. Ad *dl1520* (also known as Onyx-015) with deletion of the *E1b-55k* gene preferentially replicates in cancer cells and causes oncolysis.<sup>1</sup> The oncolytic therapy of Onyx-015 has been extensively studied in multiple clinical trials.<sup>2-4</sup> With the methods of electron microscopy and in situ hybridization to viral DNA, studies demonstrated that Onyx-015 can replicate in and destroy tumor cells at the exclusion of surrounding normal tissue in cancer patients.<sup>5,6</sup> However, limited therapeutic effect has been reported and further development of Onyx-015 was abandoned in the United States.<sup>7</sup> The rights of Onyx-015 were bought by a Chinese company, Sunway Biotech, which has completed phase III clinical studies with H101, an Ad structurally similar to Onyx-015.<sup>2</sup> The company reported a 79% positive response rate for H101 plus chemotherapy as compared with 40% for chemotherapy alone in clinical trials performed on Chinese cancer patients.<sup>2</sup> With these results, the Chinese State Food and Drug Administration approved H101 for use in combination with chemotherapy for the treatment of late-stage cancers. H101 is the

only oncolytic Ad approved as a commercial anticancer agent for cancer treatments.

The United States National Cancer Institute recommends the consumption of 5 to 9 servings of fruits and vegetables daily to reduce the risk of certain cancers. Vegetable consumption per capita is generally higher in traditional Chinese diets. It is not clear whether higher vegetable consumption may affect the outcome of Ad-mediated oncolytic therapies.

Indole-3-carbinol (I3C) is derived from glucobrassicin in brassica vegetables, such as cabbage, broccoli, cauliflower, and Brussels sprouts. Epidemiological studies suggest that high intake of cruciferous vegetables is associated with a lower risk of cancers.<sup>8</sup> Experiments conducted primarily using laboratory animals and cultured cells have shown that I3C as a dietary supplement exhibits potent anticarcinogenic properties in a wide range of cancers. When I3C was fed in the diet of A/J mice induced by tobacco smoke carcinogen, lung tumorigenesis was inhibited through inhibition of proliferation and induction of apoptosis in tumor cells.<sup>9-11</sup> Similar results were observed with mouse models of other cancers, such as breast cancer<sup>12</sup> and skin tumor.<sup>13</sup> Limited and inconclusive studies suggest that I3C may have anticarcinogenic properties in a wide range of cancers; thus it is used as a dietary supplement in the hope of cancer prevention.<sup>14-17</sup>

In the present study, we investigate the effect of I3C on cancer cell growth and Ad oncolytic replication. We observed that high doses of I3C induced cancer cell apoptosis and that low doses of

\*Correspondence to: Heshan Sam Zhou; Email: hszhou01@louisville.edu

Submitted: 04/24/2014; Revised: 06/13/2014; Accepted: 06/22/2014; Published Online: 06/27/2014  
<http://dx.doi.org/10.4161/cbt.29690>

I3C inhibited cell proliferation and caused cell cycle arrest by selective repression of cyclin E. We provide evidence showing that the combination treatment with low concentration of I3C and oncolytic Ad resulted in enhanced cytotoxic effects in cancer cells by synergistically activating apoptosis.

## Results

### High doses of I3C induce apoptotic cancer cell death

To examine the effects of I3C on cancer cell viability, human lung cancer A549 cells were treated with I3C at concentrations of 0, 200, 400, or 600  $\mu\text{M}$  for three days. The cell growth was observed daily for 3 d (Fig. 1A). Treatment with 600  $\mu\text{M}$  I3C caused cell death and nearly 100% cells became debris by day 3. However, I3C at 200  $\mu\text{M}$  did not cause significant cell morphological change during the treatment. To examine the toxicity of I3C, a cell proliferation MTT assay was performed (Fig. 1B). Cell viability was decreased after treatment with higher doses of I3C (400 and 600  $\mu\text{M}$ ), but there was no significant change in A549 cell viability after treatment with 200  $\mu\text{M}$  I3C in 3 d (Fig. 1B). Thus, I3C at concentrations at or exceeding 400  $\mu\text{M}$  resulted in toxicity in A549 cells.

To evaluate whether the cytotoxic effects of I3C at high concentrations is related with apoptosis, a dual staining approach with 7-AAD and Annexin V was conducted followed by flow cytometric analysis. We observed that A549 cells treated with 400 or 600  $\mu\text{M}$  I3C for 3 d increased both early (Annexin V-positive/7-AAD-negative) and late apoptosis (Annexin V-positive/7-AAD-positive), resulting in total 42.2% and 74.2% apoptotic cells, respectively (Fig. 1C). In contrast, cells treated with a low dose of I3C (200  $\mu\text{M}$ ) exhibited apoptosis similar to that without I3C treatment.

### Low doses of I3C inhibit proliferation of cancer cells by selectively inhibiting cell cycle-related gene expression

As no significant effect on A549 cell viability was observed in the presence of low dose of I3C (200  $\mu\text{M}$ ) for 3 d (Fig. 1), further experiments were conducted to determine if long-term treatment with low concentrations of I3C would affect A549 cell proliferation. A549 cells were treated with low concentrations of I3C (0, 50, 100, or 200  $\mu\text{M}$ ) for 28 d. To maintain cell culture conditions, I3C-treated cells were passaged weekly and then equal numbers of cells were added to fresh dishes for continual I3C treatments with the same concentrations. Cell growth inhibition by low-dose I3C was observed after 7 d and accumulation effect exhibited with increased treatment time (Fig. 2A and B). The data obtained with MTT assay confirmed that I3C long-term treatment at low doses inhibited cell growth in a dose and time dependent manner. By 28 d, treatments with 50, 100, or 200  $\mu\text{M}$  I3C decreased A549 cell viability to 90, 75 or 65%, respectively (Fig. 2B).

To evaluate whether the cell growth inhibition of low doses of I3C were due to cell cycle arrest, cells treated 14 d were stained with propidium iodide for cell cycle analysis by flow cytometry. Treatment with low doses of I3C increased cell population in the  $G_1$  phase of the cell cycle, with a concomitant reduction of cells in the S phase in a dose-dependent manner (Fig. 2C).

Flow cytometry profiles of nuclear DNA content in A549 cells revealed that  $G_1$  cell population increased from 51% to 75% and S phase cell population decreased from 36% to 22% when I3C increased from 0 to 200  $\mu\text{M}$  (Fig. 2C). Thus, while high doses of I3C induce cancer cell apoptosis (Fig. 1C), low doses of I3C inhibit proliferation of cancer cells and cause cell cycle arrest (Fig. 2C).

Activities of cyclin-dependent kinases (CDKs) are modulated by interactions with cyclins. It is well established that E-type cyclins interact with the kinase CDK2 and D-type cyclins form a complex with the kinases CDK4 or CDK6 during cell proliferation.<sup>18,19</sup> These cyclin-CDK complexes phosphorylate retinoblastoma (Rb) protein family members, leading to E2F release from Rb and regulation of cell cycle progression from the  $G_1$  phase into the S phase.<sup>20</sup> Therefore, cyclin E, cyclin D, and their related CDKs have important roles in cell proliferation. To investigate whether the I3C-caused cell cycle arrest is associated with intracellular repression of cell cycle-dependent proteins in cancer cells, western blot experiments were performed. We observed that both cyclin E and CDK2 were downregulated at 14 d of I3C treatment in a dose-dependent manner (Fig. 2D). However, no significant effect on cyclin D, CDK4, and CDK6 expression was observed. These results suggest that low dose I3C-mediated cell-cycle arrest and cell growth inhibition were associated with repression of cyclin E and its associated CDK2.

### The combination of I3C and Adhz63 synergistically inhibits viability of cancer cells

To determine the effect of I3C on Ad-mediated oncolytic therapy, A549 cells were pre-treated with various doses of I3C (0, 50, 100 and 200  $\mu\text{M}$ ) for 7 d and then infected with oncolytic Adhz63 at MOI of 2 for 72 h. The cytotoxic effect was analyzed by a crystal violet assay. I3C treatment increased Ad-mediated cell death under the condition in which I3C alone had less effects (Fig. 3).

To evaluate whether the combination effect is synergistic, A549 cells were pre-treated with I3C at concentrations ranging from 100  $\mu\text{M}$  to 300  $\mu\text{M}$  for 7 d, and then infected with Ad5, Adhz63, or AdGFP at MOI of 1. After three days infection, cells were fixed and stained with crystal violet solution. We confirmed that I3C sensitized cancer cells to Ad5 and Adhz63 infection. The relative A549 cell viability was 84% for Adhz63 treatment alone (Fig. 4B). When 300  $\mu\text{M}$  I3C was combined with Adhz63, the relative cell viability decreased to 19%. Similar results were observed when I3C was combined with Ad5, whereas I3C in combination with AdGFP, a negative control vector, did not cause any significant increased cytotoxic effect as compared with I3C alone (Fig. 4A and B).

To assess whether I3C act synergistically with Ad, we used the Chou-Talalay method,<sup>21</sup> which quantitatively describes the interaction between two or more drugs, where a CI < 1 and a CI > 1 indicate synergism and antagonism, respectively. As showed in Figure 4C, the CI values were consistently less than 1 (ranged from 0.42 to 0.95) for all concentrations of I3C in combination with Adhz63 (Fig. 4C). The results indicate that co-treatment of I3C and oncolytic Adhz63 is highly synergistic.

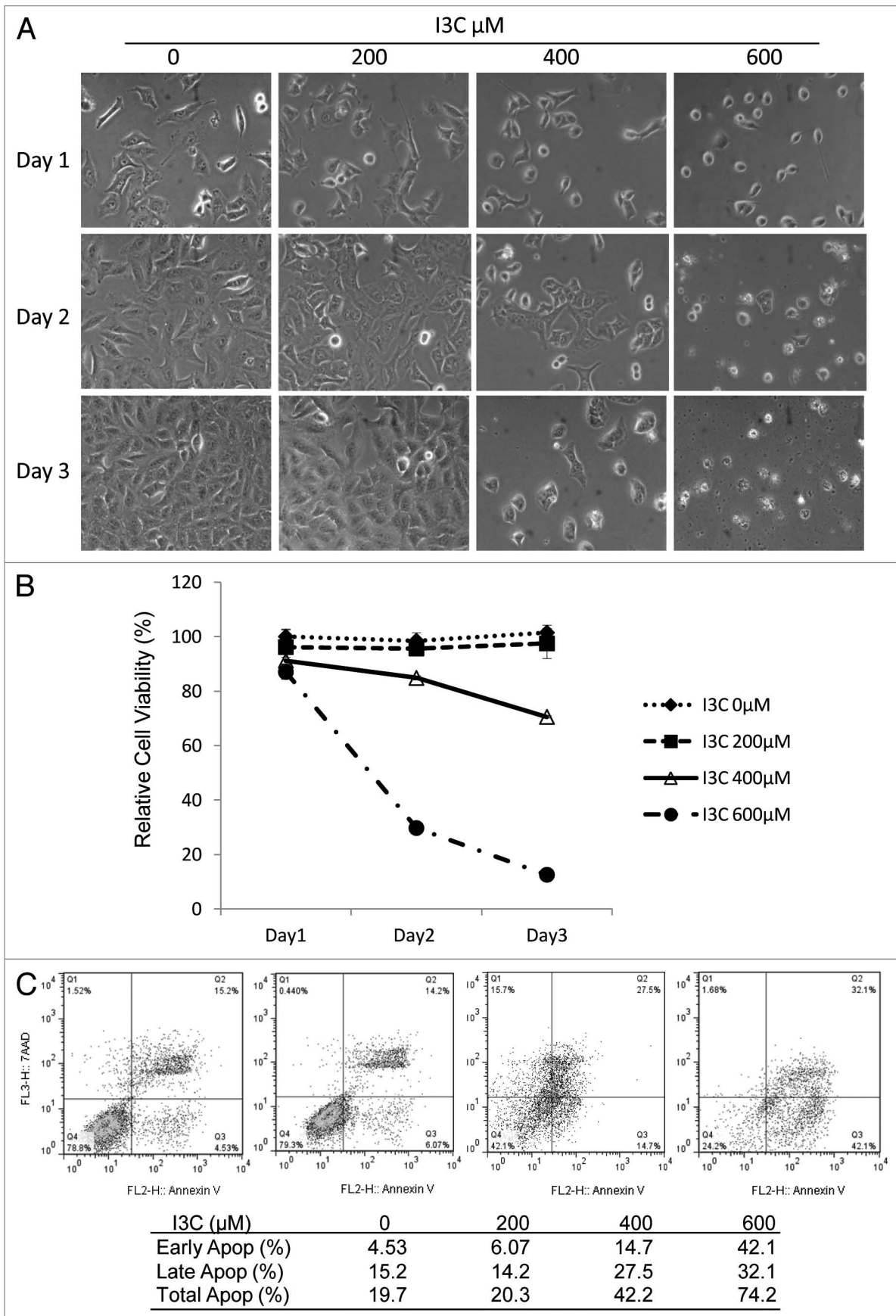


**Figure 1.** For figure legend, see page 1259.

**Figure 1 (See opposite page).** Effects of I3C on cell growth and apoptosis in A549 cells. Cells were treated with increasing doses of I3C (0–600  $\mu$ M) for 3 d. **(A)** Comparison of cell proliferation in A549 cells. **(B)** Comparison of cell relative viabilities in A549 cells. Cell viability was estimated by MTT assay as described in Materials and Methods. **(C)** Comparison of apoptosis induction in A549 cells. Flow cytometry analysis was performed using a dual staining approach with 7-AAD and Annexin V.

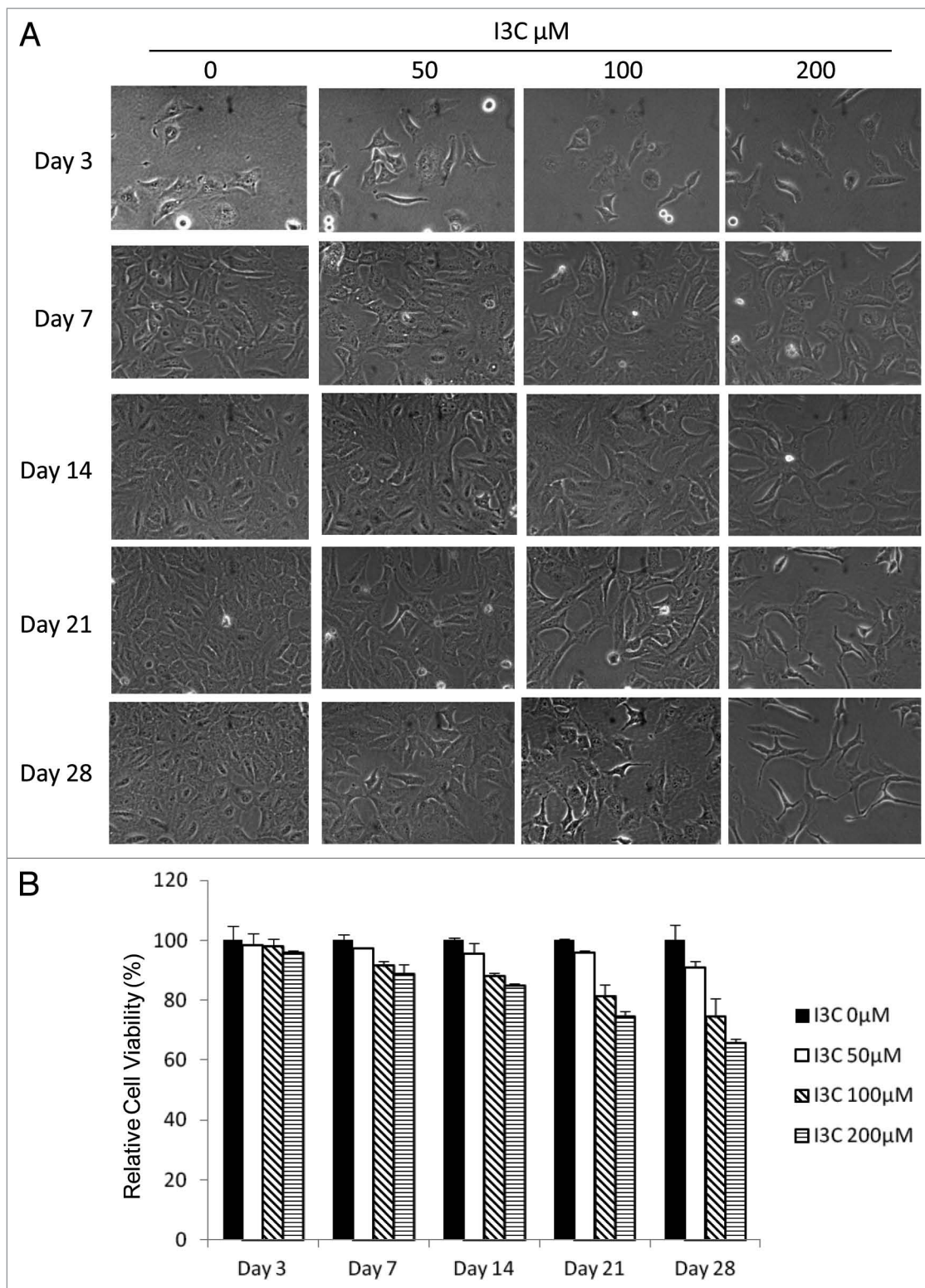


**Figure 2A and B (For C and D, see page 1260).** Effects of I3C at low doses on A549 cells. **(A)** Comparison of cell proliferation in A549 cells treated with increasing doses of I3C (0–200  $\mu$ M) for various days. **(B)** Comparison of cell relative viabilities in A549 cells. Cell viability was estimated by MTT assay.

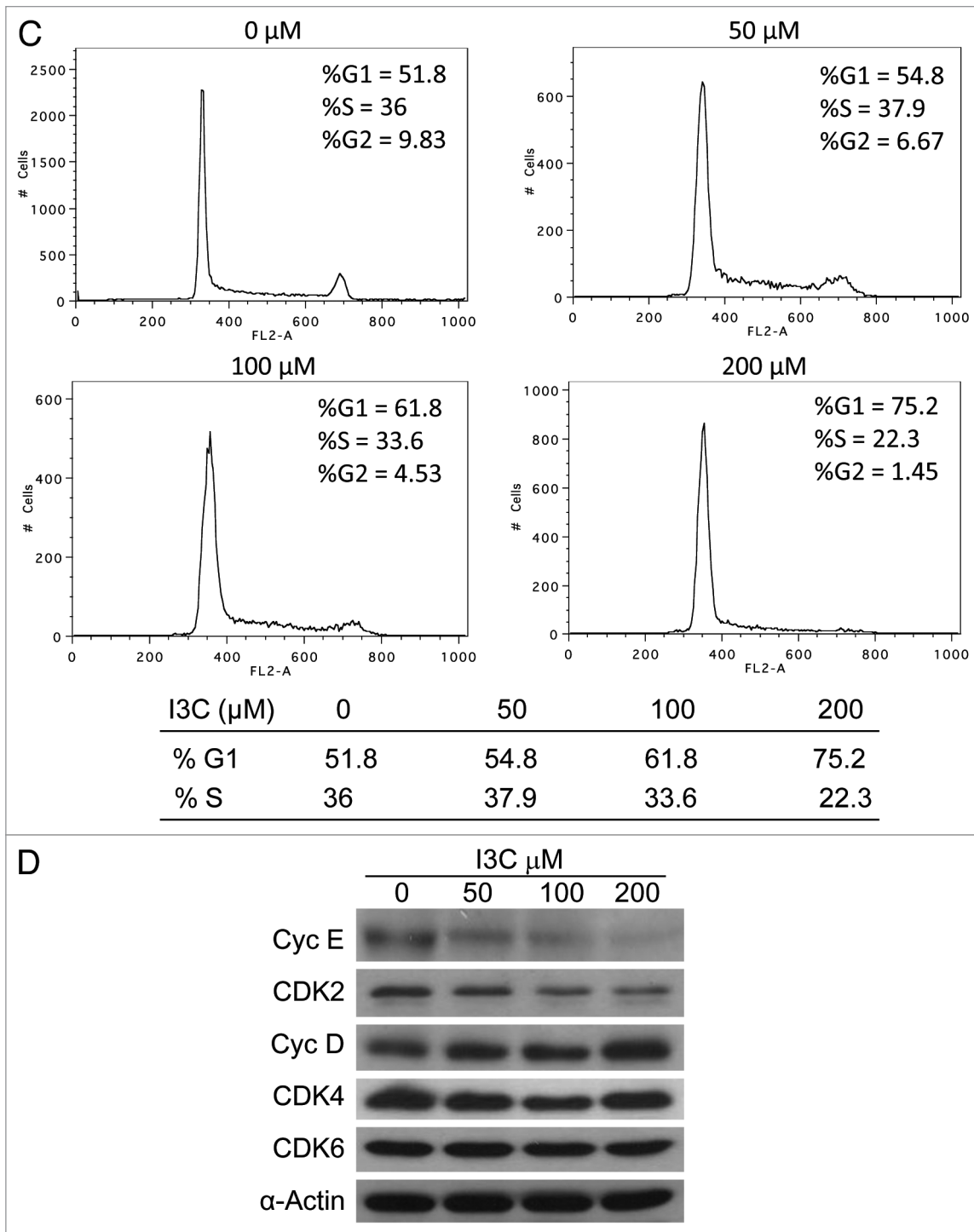


**Figure 2C and D (For A and B, see page 1259).** Effects of I3C at low doses on A549 cells. **(C)** Comparison of the I3C effects on cell cycle. Cells were exposed to I3C (0, 50, 100, or 200 μM) for 14 d, and then stained with propidium iodide and analyzed for DNA content by flow cytometry. **(D)** Effects of I3C on expression of cell cycle related proteins. Cells were exposed to increasing doses of I3C (0–200 μM) for 14 d. G<sub>1</sub> cell cycle related proteins were analyzed by immunoblot analysis using specific antibodies against cyclin E, cyclin D, CDK2, CDK4, CDK6 and α-actin.

To ensure that the observed effect was not limited to this specific cell line, we also tested other cancer cell lines with combination treatment of I3C and Adhz63 at MOI 1 and 2. In addition to A549 cells, we also observed that virus treatments alone in this condition exhibited minimally toxic to H1299,

RKO, and HCT116 cells (Fig. 5). As we expected, enhanced antitumor effect against these cancer cell lines with combination treatment was observed. These results indicate that I3C can enhance Ad oncolytic therapy with different types of cancer cells.

### Combinational treatment with I3C and Adhz63 results in synergistic activation of apoptosis

To study the mechanism of I3C-enhanced Ad oncolytic cytotoxicity, we examined whether the combination cytotoxic effects of I3C and Adhz63 were due to increased apoptosis in cancer cells. A dual staining approach with 7-AAD and Annexin V was conducted followed by flow cytometric analysis. A549 cells were pre-treated with 200  $\mu$ M I3C for 7 d and then infected with Adhz63 at a MOI of 1 for three days. I3C alone and Adhz63 alone did not affect A549 early and late apoptosis significantly (Fig. 6A). However, the combination treatment of I3C and Adhz63 increased total apoptosis 2-fold from 18.3% to 36.6%. Notably, the early apoptosis was increased 5-fold from 3.2% for the mock control to 15.7% for the combination treatment (Fig. 6A).

One of the earliest and most consistently observed features during the execution phase of the apoptotic process is the activation of caspases, a family of cysteine proteases.<sup>22</sup> Caspase 9, the prime initiator protease, is activated during the mitochondria-mediated apoptosis pathway and triggers a cascade of caspase-activation. To study the I3C and Adhz63 cotreatment-induced apoptosis in cancer cells, caspase 9 activities were determined by caspase-9 colorimetric assay. Without Ad infection, caspase-9 activity in A549 cells was not affected by I3C at the doses of 100 and 200  $\mu$ M. However, Adhz63 infection increased A549 cell caspase-9 activity that was further enhanced by I3C, indicating the combinational efficacy of I3C and Adhz63 (Fig. 6B).

The activation of caspase cascade requires a series of proteolytic processing in caspases.<sup>22</sup> Thus, we further examined the proteolytic cleavage of initiator caspase-9, effector caspase 3, and the cellular target nuclear enzyme poly (ADP-ribose) polymerase (PARP).<sup>23</sup> Figure 6C showed that combination of lower doses of I3C and 1 MOI Adhz63 increase the levels of cleaved caspase 9, 3, and PARP as compared with I3C and virus treatment alone (Fig. 6C). Taken together, these results show that I3C enhances Ad cytotoxic effects by increasing apoptotic caspase activation.

### I3C reduces adenoviral replication likely by inhibiting cyclin E

We further investigated whether I3C may affect Ad replication. Our previous studies have shown that Ad infection induces cyclin E expression<sup>24,25</sup> that activates CDK2 for efficient viral replication.<sup>26</sup> As cyclin E and CDK2 play an important role in Ad replication, inhibition of cyclin E and CDK2 by I3C treatment may affect Ad oncolytic replication. We first evaluated I3C effect on cyclin E and CDK2 protein levels in A549 cells infected with Adhz63. In this experiment, A549 cells were cultured in medium without I3C or with I3C at concentrations of 100, 200, and 300  $\mu$ M for 7 d, and then infected with Adhz63 at 1 MOI for 1 and 3 d. Cyclin E protein levels, but not CDK2, were repressed in Adhz63-infected A549 cells pretreated with I3C (Fig. 7A).

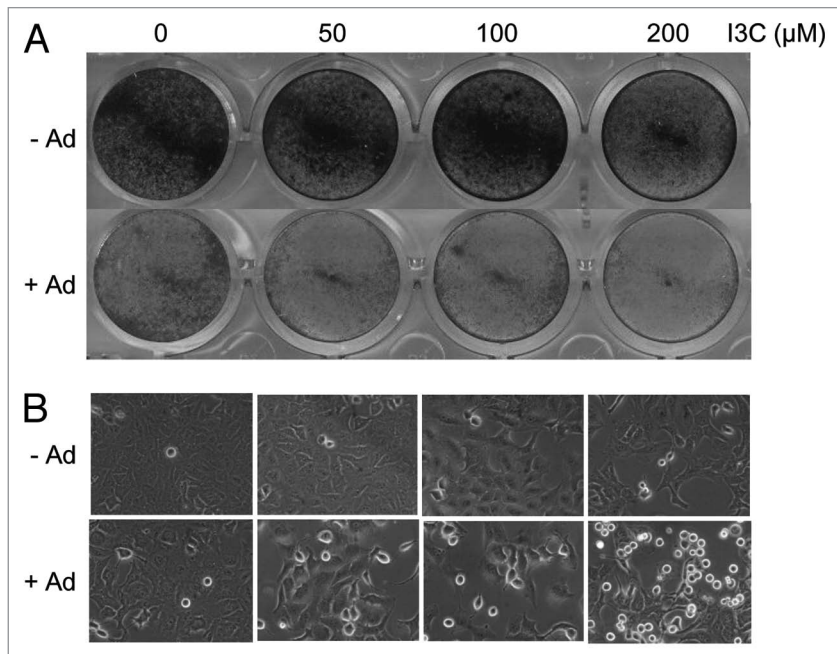


**Figure 3.** Effects of combination of I3C and oncolytic Adhz60 on A549 cells. A549 cells were pre-treated with various concentrations of I3C for 7 d and then infected with oncolytic Ad or without virus for three days. (A) Cell viabilities were analyzed using crystal violet staining. (B) Comparison of cell proliferation in A549 cells.

We further investigated the effect of I3C on Adhz63 replication. In this experiment, A549 cells were pre-treated with I3C at concentrations of 200  $\mu$ M for 7 d, and then infected with Ad5 or Adhz63 at MOI of 1 for 3 d in the presence of I3C. After infection, viral titers were determined. Without I3C treatment, the titers of Ad5 and Adhz63 were increased to  $2 \times 10^8$  and  $7 \times 10^7$  infect units (IFU)/mL in 3 d, respectively (Fig. 7B). I3C treatment repressed Ad5 and Adhz63 replication; Ad5 titers decreased 5-fold from  $2 \times 10^8$  to  $4 \times 10^7$  IFU and Adhz63 titers decreased 18-fold from  $7 \times 10^7$  to  $4 \times 10^6$  IFU (Fig. 7B). Consistently, the production of Adhz63 viral capsid proteins was also inhibited in the presence of I3C (Fig. 7C). These results suggest that I3C may partially reduce adenoviral replication by repressing cyclin E expression.

## Discussion

In the present study, we have shown that high doses of I3C induced cancer cell death associated with increased apoptosis and low doses of I3C inhibited cell growth by repressing cyclin E expression. We also observed that I3C can sensitize cancer cells to Ad-mediated oncolysis.

It has been reported that high intake of vegetables may be associated with a lower risk of cancer.<sup>8</sup> Limited and inconclusive studies suggest that I3C, a naturally occurring compound derived from cruciferous vegetables, may have a variety of anti-cancer properties.<sup>14</sup> In our study, we observed that high doses of I3C ( $\geq 400$   $\mu$ M) directly destroyed cells in 3 d after the treatment. We further found that no obvious cytotoxic effect was observed

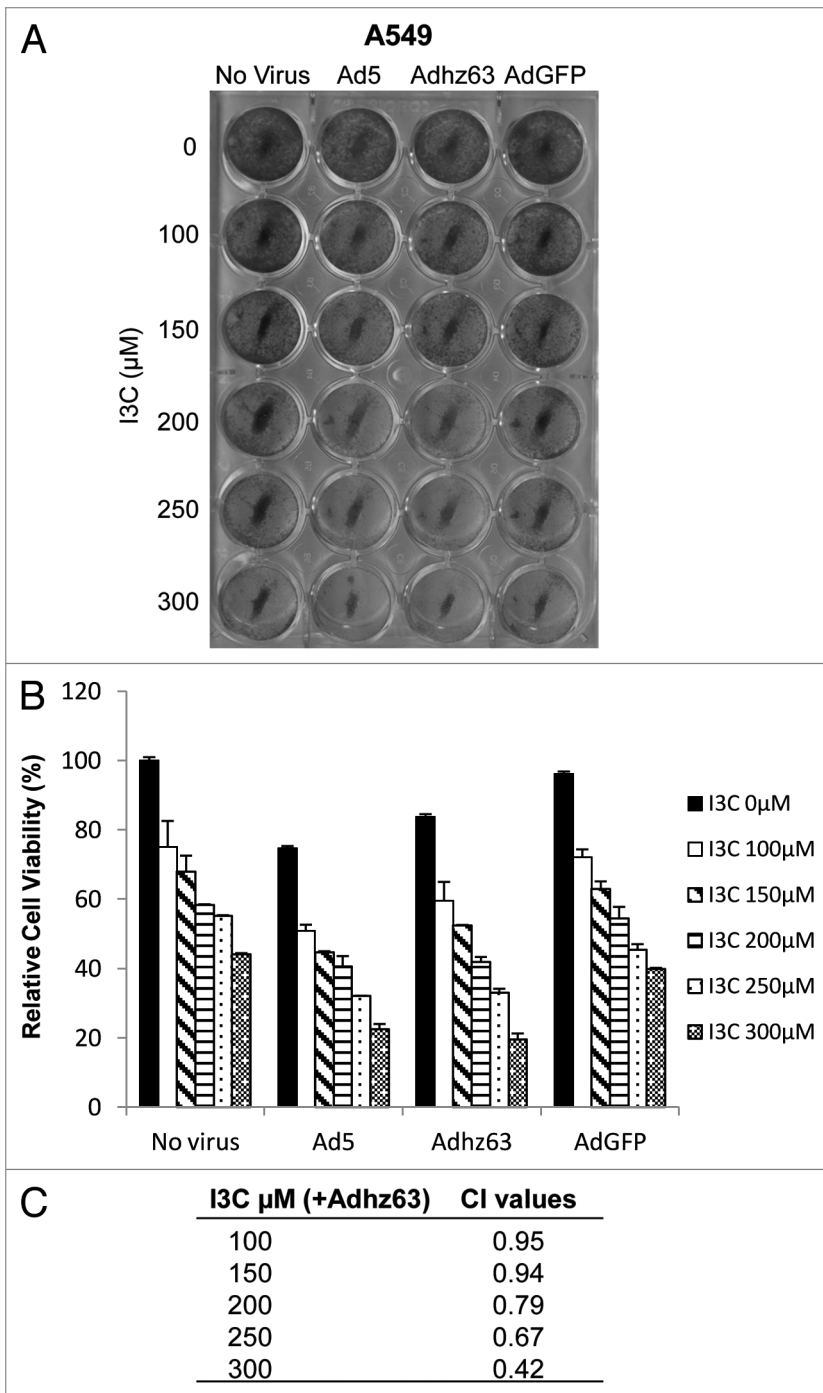


**Figure 4.** Effects of combination of I3C and Adhz63 on A549 cell viability. **(A)** Cell viabilities were measured using crystal violet staining. A549 cells were pre-treated with various concentrations of I3C for 7 d and then infected with Ad5, Adhz63, AdGFP, or without virus for three days. **(B)** The dye retained by the adherent cells was solubilized with 2% SDS, and absorbance was recorded at 590 nm. Cell viability was expressed as the amount of dye in treated cells relative to that of untreated control cells. **(C)** The combined effects of I3C and Ad viruses were evaluated by combination index (CI) using the CalcuSyn software (Biosoft). CI = 1 indicates additivity; CI < 1 represents synergism, and CI > 1 indicates antagonism.

with low doses of I3C ( $\leq 200 \mu\text{M}$ ) after long-term treatments (2–4 wk). Lower doses of I3C have an anti-proliferative effect that was due to cell cycle arrest, accompanied by selective repression

of cyclin E and its related CDK2. Cyclin E has two notable functions, controlling the entry into the S phase of the cell cycle and increasing DNA replication.<sup>27,28</sup> Expression of cyclin E is strictly controlled in normal cells. The level of cyclin E rises at late G<sub>1</sub> phase, peaks at the G<sub>1</sub>/S phase to promote the S phase entry, and decreases thereafter.<sup>29,30</sup> Ectopic overexpression of cyclin E causes cell-cycle anomalies and genetic instability.<sup>31–33</sup> Cyclin E over-activation likely relaxes the strict control of the G<sub>1</sub>/S transition, increases cell proliferation and DNA replication, leading to the accumulation of gene mutations. Cancer cells are frequently associated with cyclin E overexpression or dysregulation. Transgenic cyclin E was shown to trigger dysplasia and multiple pulmonary adenocarcinomas in transgenic mouse lung cancer models.<sup>34</sup> In the current study, we demonstrated for the first time that prolonged exposure of I3C at low doses repressed cyclin E and its associated CDK2 expression and decreased cell growth (Fig. 2). The cellular consequence of I3C-repressed cyclin E expression and cell proliferation allow cells to repair their mutations and prevent tumorigenesis. Promising chemopreventive agents should have greater antitumor efficacy without adverse effect. Our findings suggest that long-term use of low doses of I3C may safely prevent cancer development by repressing cyclin E and its partner CDK2 activity without obvious adverse effect.

Oncolytic Ads as a single anticancer agent cannot effectively eradicate tumors in clinical studies.<sup>35,36</sup> One possible explanation is that some cancer cells within tumors may be resistant to oncolytic Ad replication. To complete the tumor eradication, oncolytic Ads have been tested in conjunction with standard treatments of chemotherapy and radiation therapy. Combinational therapies have shown enhanced therapeutic effects in vitro and in vivo compared with monotherapy.<sup>37,38</sup> There have been no prior reports of the benefit of dietary supplements to oncolytic virotherapy. In the current study, we discovered synergistic effects of combination of I3C with oncolytic Ads. *E1b55K*-deleted Ads have been tested in clinical trials and achieved limited success. By far Onyx-015 has not been approved for commercial applications in cancer treatments. However, a structurally similar vector H101 seems having achieved therapeutic responses in clinical trials in China and has thus been approved as a commercial anticancer agent for clinical applications.<sup>4</sup> In consideration of diet traditions, cancer patients in China likely consume more vegetables and compounds in vegetables may affect the outcomes of virotherapies. In the present study, we show that low doses of I3C enhanced Ad oncolysis synergistically

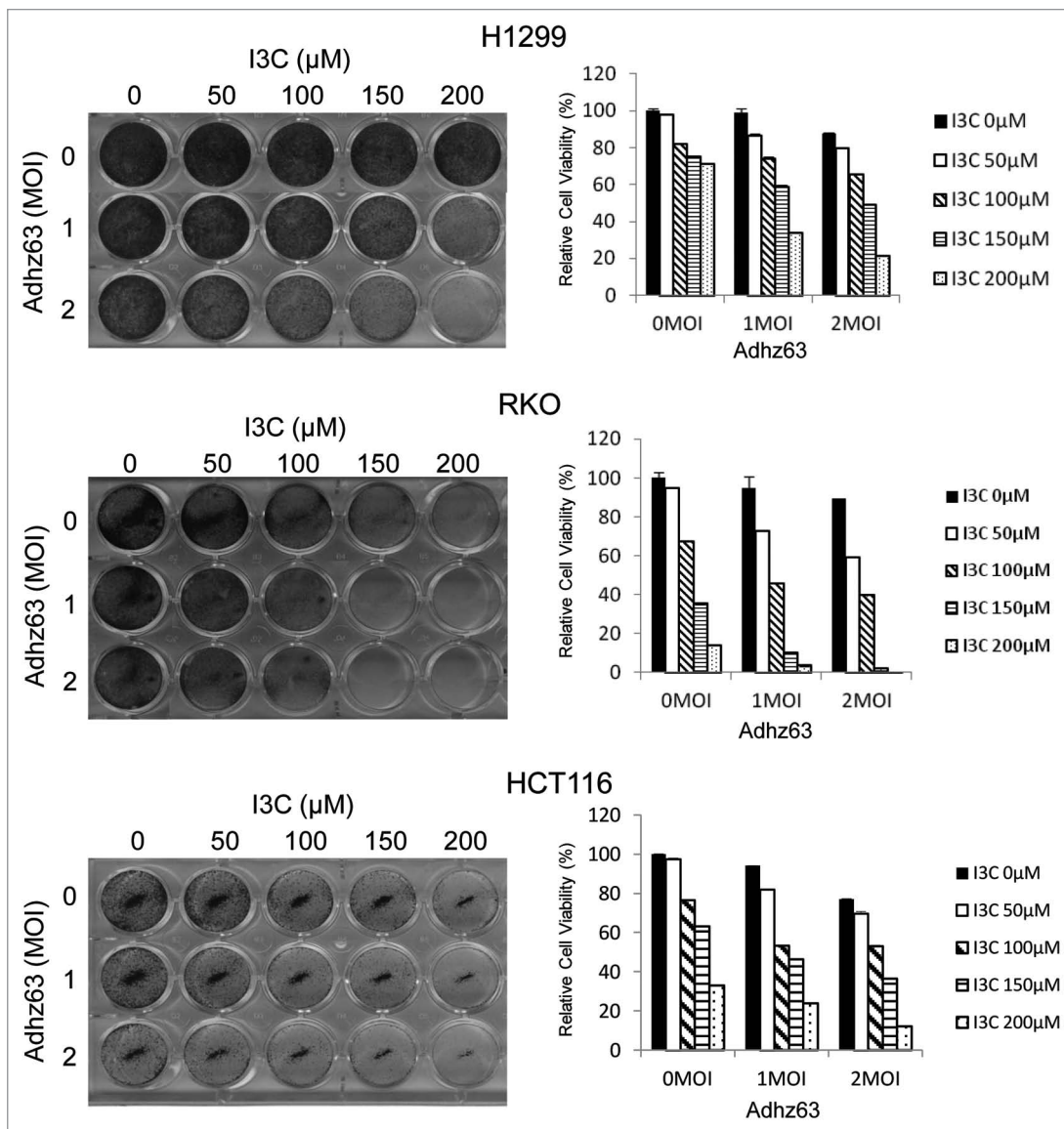


**Figure 5.** Effects of I3C and Adhz63 on H1299, RKO, and HCT116 cell viability. Cell viabilities were measured using crystal violet staining. Cells were pre-treated with various concentrations of I3C for 7 d and then infected with Adhz63 or without virus infection for 3 d. The dye retained by the adherent cells was solubilized with 2% SDS, and absorbance was recorded at 590 nm. Cell viability was expressed as the amount of dye in treated cells relative to that of untreated control cells.

by promoting cancer cell apoptosis (Figs. 4 and 5). The upregulation of caspase 9 activities and cleavage of caspase 9, 3, and PARP occurred in I3C-dose dependent manner in the cells infected with Adhz63 (Fig. 6). Our results for the first time indicate that I3C can sensitize cancer cells to Ads-induced cancer cell death and that apoptosis events triggered by the combination of I3C and oncolytic Ads may play a critical role in the synergistic antitumor effect. We did not observe increased autophagy in cancer cells after the combinational treatment with I3C and Ads. We have previously shown that autophagy increases adenovirus replication by degrading intracellular components for building progeny virus particles.<sup>39</sup> Therefore, autophagy is unlikely to play an important role in I3C-reduced Ad replication.

A phase I clinical trial studied tolerability and effects of I3C in women.<sup>40</sup> In the study, subjects ingested 400 mg I3C daily for 4 wk followed by a 4-wk period of 800 mg I3C daily. These chronic doses were tolerated well by all subjects. In our in vitro experiments, cancer cells were treated with I3C at concentrations 50, 100, or 200  $\mu$ M for 28 d. 100  $\mu$ M I3C is 14.746 mg/L or about 737 mg in 50 Kg solution, which is within the range of I3C doses used in the clinical trial. However, the concentrations used in in vitro experiments cannot be easily converted to dosages for in vivo and clinical studies because these are more complicated and we have to consider many factors, such as drug bioavailability and distribution. Thus, animal studies are necessary to further investigate the clinical relevance.



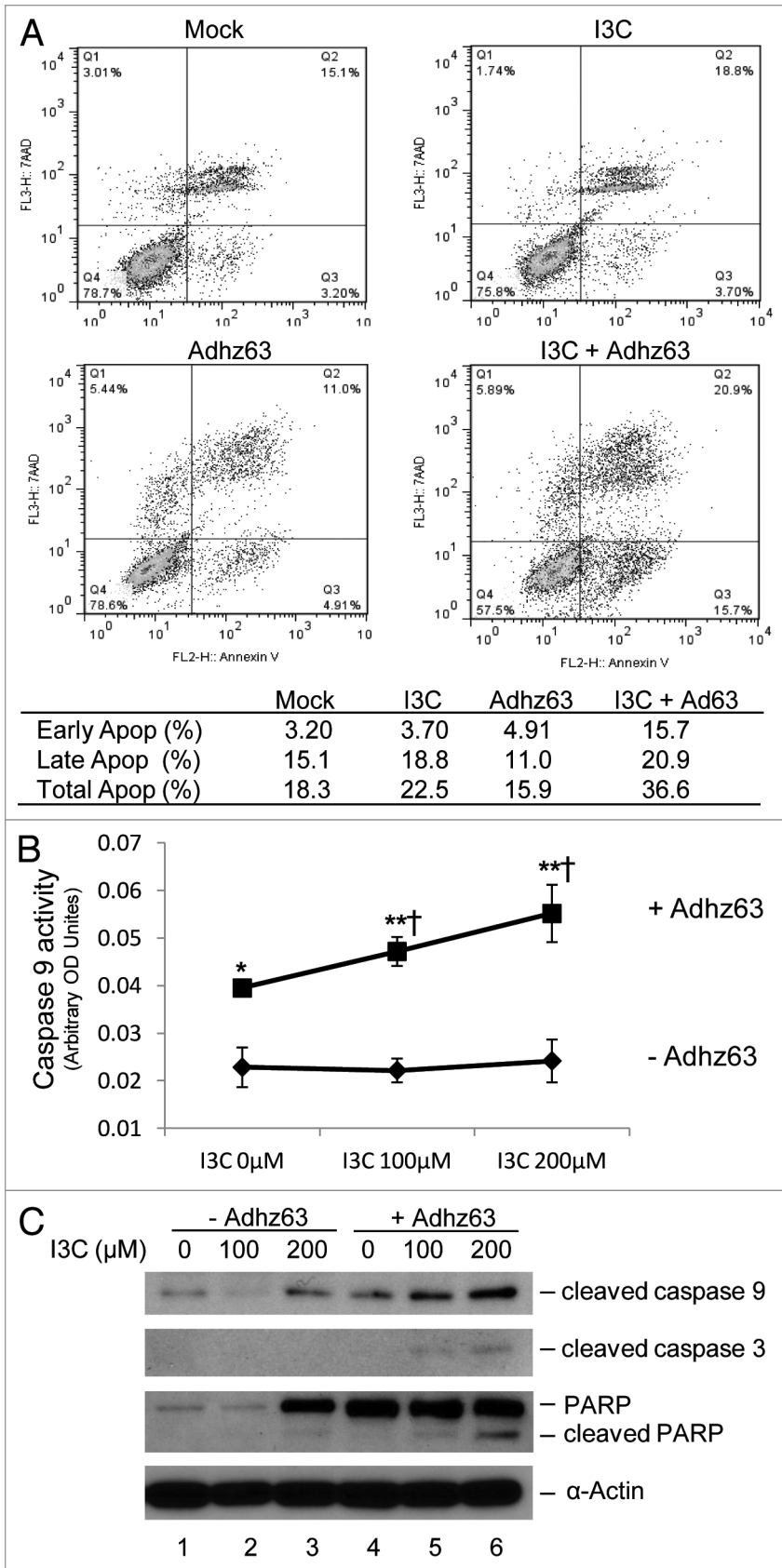


**Figure 6.** Effects of combination of I3C and Adhz63 on induction of apoptosis in A549 cells. Cells were pre-treated with I3C for seven days and then infected with Adhz63 at a MOI of 1 for three days. **(A)** Flow cytometry analysis was performed using a dual staining approach with 7-AAD and Annexin V for detection of co-treatment induced apoptosis. **(B)** Caspase 9 activities were determined by caspase-9 Colorimetric Assay. Co-treatment of I3C and Adhz63 vs. I3C alone control correspondence ( $*P < 0.05$ ,  $**P < 0.001$ ); vs. Adhz63 alone control ( $†P < 0.05$ ). **(C)** The protein levels of cleaved caspase 9, caspase 3, and PARP in A549 cells were determined by western blot analysis.

cyclin E.<sup>24</sup> E1B55K-deleted Ads fail to induce cyclin E expression in normal cells and therefore their replication is restricted.<sup>25</sup> However, *E1b55K*-deleted oncolytic Ads can still efficiently induce cyclin E in cancer cells with dysregulated cyclin E and carry out sufficient oncolytic replication.<sup>25,26</sup> In this study, we observed that expression of cyclin E was downregulated in response to the treatment with I3C. As a consequence of repression of cyclin E induction, pre-treatment with I3C repressed replication of Ads up to 10-fold (Fig. 7). These results support the hypothesis that cyclin E induction is critically important for Ad replication. Although I3C reduces oncolytic Ad replication, the combination treatment still elicits synergistic antitumor effects.

In summary, our results uncovered for the first time that I3C enhances cytotoxic effects of oncolytic Ads by synergistic activation of apoptosis. We also demonstrated that I3C had antitumor effects by induction of apoptosis and by repression of cyclin E and cell proliferation depending on the concentration used in the assays. Our findings provide a novel rationale for the clinical potential of I3C in cancer prevention and in Ad oncolytic therapies. The combination of I3C and oncolytic Ads should be further studied to evaluate the efficacy and safety in animal experiments.

## Materials and Methods

### Cell lines and culture conditions

HEK 293 (ATCC® CRL-1573™), human lung cancer A549 (ATCC® CCL185™) and H1299 (ATCC® CRL-5803™), human colon cancer RKO (ATCC® CRL-2578™) and HCT 116 (ATCC® CCL-247™) cell lines were purchased from the American Type Culture Collection. A549 cells were grown in MEM-Alpha medium; H1299 and RKO were cultured in RPMI1640 medium, HCT116 in McCoy's 5a Medium and 293 was grown in DMEM

We previously have reported that Ad E1B55K protein is involved in the induction of cell cycle-related genes, including

HCT116 in McCoy's 5a Medium and 293 was grown in DMEM

**Figure 7.** Effects of combinations of I3C and Adhz63 on expression of cyclin E and CDK2 in A549 cells. **(A)** Cells were pre-treated with various concentrations of I3C for 7 d and then infected with Adhz63 at a MOI of 1. Cyclin E and CDK2 protein levels in A549 were determined by western blot analysis with specific antibodies. **(B)** The virus titers were determined at days 1, 2 and 3 post-infection with the infection unit method. **(C)** The viral capsid proteins were determined by western blotting with a rabbit-anti-Ad protein virions antibody.

medium at subconfluence at 37 °C in humidified air containing 5% CO<sub>2</sub>. All media were supplemented with 10% heat-inactivated fetal bovine serum, 2 mM L-glutamine, and penicillin/streptomycin (100 U/mL). All cell culture reagents were obtained from Gibco BRL and Corning Cellgro.

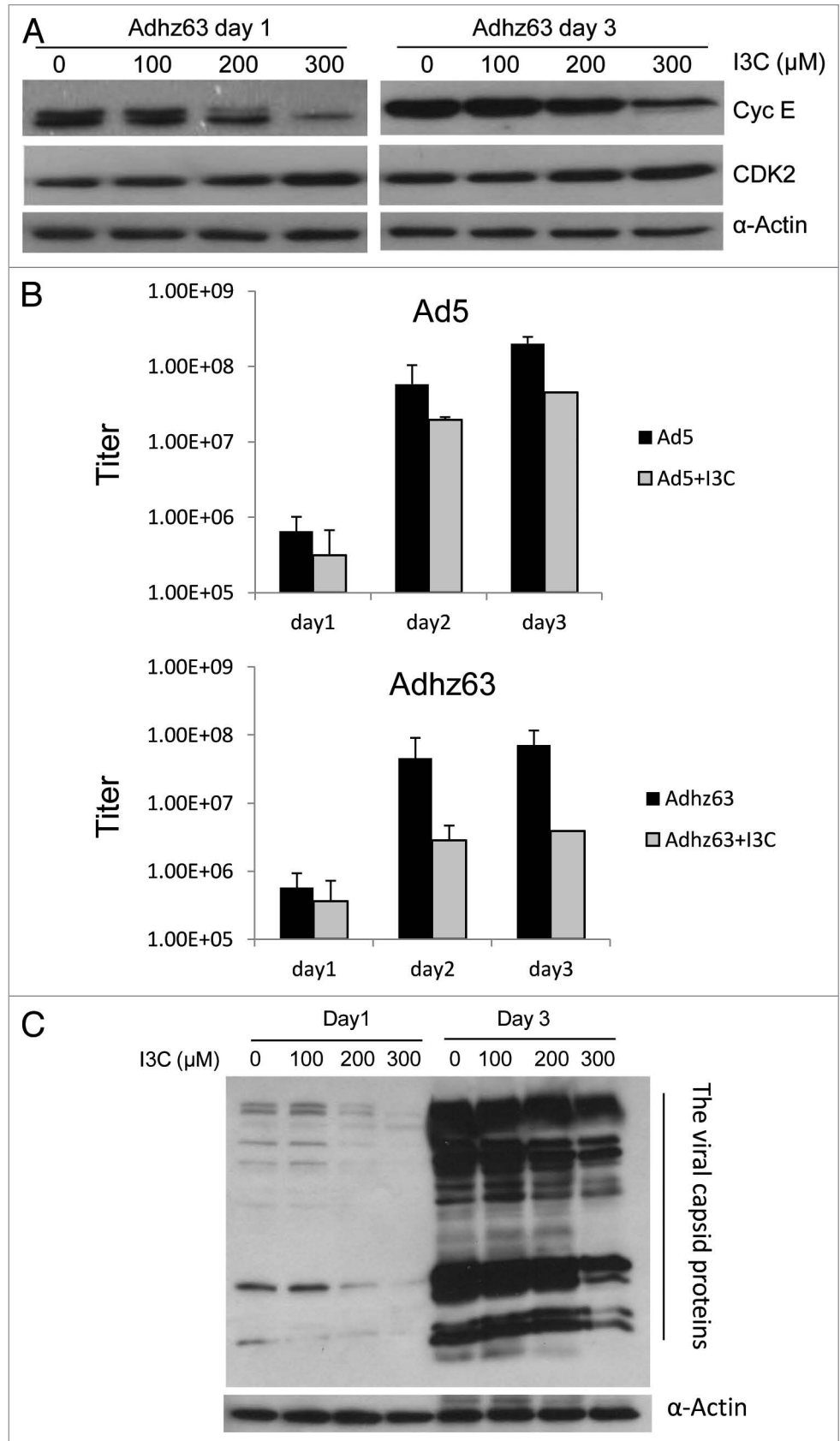
#### Adenoviral vectors and titration

Wild-type Ad type 5 (Ad5, ATCC no. VR-5) was used as a replication-competent control. AdGFP, an Ad vector with *E1* deletion carrying a green fluorescent protein (GFP), was used as a replication-defective control. Adhz63 is an oncolytic Ad vector constructed by our laboratory with the deletion of E1B55K region similar to dl1520.<sup>41</sup> All of the vectors created and used in this study are based on the backbone of Ad5. Total infected cells and culture supernatants were collected at the indicated time points and lysed to release virus particles with three cycles of freezing and thawing. The viral titers were determined by the infective unit method as described previously.<sup>42,43</sup> Briefly, HEK 293 cells were seeded in 96-well plates at a density of 10<sup>3</sup> (cells/well) and then infected with 10-fold serially diluted viruses. CPE was recorded and scored after incubation for 7 d.

#### Cell proliferation assay

Growth inhibition of I3C was evaluated using a 3-[4,5-dimethylthiazol-2-yl]-2,5-diphenyltetrazolium bromide (MTT) assay. This assay quantifies viable cells by measuring the conversion of the

3-(4,5-dimethylthiazol-2-yl)-2,5-diphenyltetrazolium bromide (MTT) to purple formazan, according to the manufacturer's



instructions (Boehringer Mannheim). The absorbance of the supernatant was measured at 590 nm using a Synergy HT Multi-Mode Microplate Reader (Bio-Tek). Based on the absorbance of the cell samples, cell viability can be measured. Cell viability was expressed as the amount of dye reduction in treated cells relative to that of untreated control cells. The data are presented as the mean  $\pm$  SD of triplicate samples from at least three separate representative experiments and were analyzed by the Student *t* test.

#### Crystal violet cell viability assay

The cytotoxic effect of drug combination of I3C and Adhz63 was analyzed by a crystal violet assay.<sup>44</sup> After the culture medium was removed, cells were fixed with 3.7% Paraformaldehyde for 10 min and then carefully washed with PBS. Cells were incubated in a solution of 1% crystal violet in distilled water for 15 min at room temperature, followed by washing with tap water until excess color was removed and then set to air dry. Images were scanned with HP Scanjet 4070 Photosmart Scanner. The dye retained by the adherent cells was solubilized with 2% SDS, and absorbance was recorded at 590 nm with a Synergy HT plate reader (BioTek). The OD values were quantitated into the cell viability % by the formula, cell viability % = (OD value of experimental group / OD value of control group)  $\times$  100%. The mock-control group was calculated as 100% of cell viability in the assay.<sup>45</sup> The data obtained from the assay were also analyzed by combination index (CI) method using the CalcuSyn software (Biosoft), based on the principle of Chou and Talalay.<sup>21</sup> CI = 1 indicates additivity; CI < 1 represents synergism and CI > 1 indicates antagonism.

#### Flow cytometric analysis of DNA content

For cell cycle analysis, the CycleTEST™ PLUS DNA Reagent Kit (BD Biosciences) was used according to the manufacturer's instructions. In brief, human lung cancer cells were plated onto 60 mm tissue culture dishes and treated with different concentrations (0, 50, 100, and 200  $\mu$ M) of I3C. After 14 d, cells were harvested. Cell nuclei were isolated and stained with a solution containing propidium iodide. Acquisition and analysis were performed by FACScan flowcytometer using Cell Quest pro software with excitation between 580 and 650 nm.

#### Flow cytometric analysis of apoptosis

For detecting apoptosis, PE Annexin V Apoptosis Detection Kit I (BD Pharmingen) was used according to the manufacturer's protocol. Briefly, to induce apoptosis, A549 cells were treated with I3C at different concentrations and 1 MOI of Adhz63, individually or in combination. Cells were harvested and washed twice with cold PBS. A total of  $1 \times 10^5$  cells were then stained with 5  $\mu$ L of PE Annexin V and 5  $\mu$ L of 7-AAD for 15 min at RT

(25 °C) in the dark, followed by flow cytometric analysis using Cell Quest pro software.

#### Measurement of caspase-9 activity

The activation of caspase 9 in A549 cells treated with different concentrations (0  $\mu$ M, 100  $\mu$ M, and 200  $\mu$ M) of I3C and 1 MOI of Adhz63, individually or in combination, was assessed using Caspase-9 Colorimetric Assay (R&D Systems, Inc.). Briefly, cells were first lysed to collect their intracellular contents. Cell lysate was then incubated with 5  $\mu$ L of caspase-9 colorimetric substrate (LEHD-pNA) in a 96-well microplate at 37 °C for 1–2 h. Colorimetric readings were performed on a microplate reader using a wavelength of 405 nm. The data are presented as the mean  $\pm$  SD of triplicate samples from at least three separate representative experiments and were analyzed by the Student *t* test. *P* < 0.05 was considered significant.

#### Western immunoblot analysis

After indicated treatments, protein isolated from A549 cells were harvested at different time points for western blot analysis. Protein concentration was measured with the BCA protein assay kit (Pierce). Fifty micrograms of protein was resolved by 10% sodium dodecyl sulfate PAGE and then electrophoretically transferred to PVDF membrane. Rainbow marker was used as the molecular weight standard. Membranes were blocked in 10% non-fat dry milk in 1 $\times$  TBST over night at 4 °C. The membranes were incubated first with the following primary antibodies: anti-cyclin D, anti-cyclin E, anti-CDK2, anti-CDK4, anti-CDK6, anti-cleaved caspase 9, anti-cleaved caspase 3, anti-poly (ADP-ribose) polymerase (PARP), anti-cleaved PARP, or anti-viral capsid proteins antibodies. Blots were subsequently incubated with goat anti-rabbit or goat anti-mouse horseradish peroxidase conjugated secondary antibodies. Electrochemiluminescent western blot analysis system (GE Healthcare) was used to visualize the signals according to the manufacturer's instructions. The proteins were detected by autoradiography. Equal protein loading was ascertained by the level of  $\alpha$ -actin protein probed with anti- $\alpha$ -actin antibody.

#### Disclosure of Potential Conflicts of Interest

No potential conflicts of interest were disclosed.

#### Acknowledgments

This work was supported by NIH Grant R01 CA129975 (H.S.Z.). P.H.C. is partially supported by the KC Huang Scholarship from the University of Louisville. We thank the other members in our laboratory for their help in the experiment: Stephen L Wechman, Jorge G Gutierrez, Hongying Hao, and Deyi Xiao.

#### References

1. Russell SJ, Peng KW, Bell JC. Oncolytic virotherapy. *Nat Biotechnol* 2012; 30:658-70; PMID:22781695; <http://dx.doi.org/10.1038/nbt.2287>
2. Garber K. China approves world's first oncolytic virus therapy for cancer treatment. *J Natl Cancer Inst* 2006; 98:298-300; PMID:16507823; <http://dx.doi.org/10.1093/jnci/djj111>
3. Kirn DH. Redemption for the field of oncolytic virotherapy. *Mol Ther* 2011; 19:627-8; PMID:21455205; <http://dx.doi.org/10.1038/mt.2011.45>
4. Yu W, Fang H. Clinical trials with oncolytic adenovirus in China. *Curr Cancer Drug Targets* 2007; 7:141-8; PMID:17346105; <http://dx.doi.org/10.2174/156800907780058817>
5. McCormick F. Cancer-specific viruses and the development of ONYX-015. *Cancer Biol Ther* 2003; 2(Suppl 1):S157-60; PMID:14508094
6. Kirn D, Martuza RL, Zwiebel J. Replication-selective virotherapy for cancer: Biological principles, risk management and future directions. *Nat Med* 2001; 7:781-7; PMID:11433341; <http://dx.doi.org/10.1038/89901>
7. Liu TC, Kirn D. Gene therapy progress and prospects cancer: oncolytic viruses. *Gene Ther* 2008; 15:877-84; PMID:18418413; <http://dx.doi.org/10.1038/gt.2008.72>

8. Higdon JV, Delage B, Williams DE, Dashwood RH. Cruciferous vegetables and human cancer risk: epidemiologic evidence and mechanistic basis. *Pharmacol Res* 2007; 55:224-36; PMID:17317210; <http://dx.doi.org/10.1016/j.phrs.2007.01.009>
9. Morse MA, LaGreca SD, Amin SG, Chung FL. Effects of indole-3-carbinol on lung tumorigenesis and DNA methylation induced by 4-(methylnitrosamino)-1-(3-pyridyl)-1-butanone (NNK) and on the metabolism and disposition of NNK in A/J mice. *Cancer Res* 1990; 50:2613-7; PMID:2328487
10. Kassie F, Matisse I, Negia M, Upadhyaya P, Hecht SS. Dose-dependent inhibition of tobacco smoke carcinogen-induced lung tumorigenesis in A/J mice by indole-3-carbinol. [Phila Pa]. *Cancer Prev Res (Phila)* 2008; 1:568-76; PMID:19139007; <http://dx.doi.org/10.1158/1940-6207.CAPR-08-0064>
11. Kassie F, Kalscheuer S, Matisse I, Ma L, Melkamu T, Upadhyaya P, Hecht SS. Inhibition of vinyl carbamate-induced pulmonary adenocarcinoma by indole-3-carbinol and myo-inositol in A/J mice. *Carcinogenesis* 2010; 31:239-45; PMID:19625346; <http://dx.doi.org/10.1093/carcin/bgp174>
12. Jump SM, Kung J, Staub R, Kinseth MA, Cram EJ, Yudina LN, Preobrazhenskaya MN, Bjeldanes LF, Firestone GL. N-Alkoxy derivatization of indole-3-carbinol increases the efficacy of the G1 cell cycle arrest and of I3C-specific regulation of cell cycle gene transcription and activity in human breast cancer cells. *Biochem Pharmacol* 2008; 75:713-24; PMID:18023427; <http://dx.doi.org/10.1016/j.bcp.2007.09.024>
13. Srivastava B, Shukla Y. Antitumour promoting activity of indole-3-carbinol in mouse skin carcinogenesis. *Cancer Lett* 1998; 134:91-5; PMID:10381134; [http://dx.doi.org/10.1016/S0304-3835\(98\)00247-X](http://dx.doi.org/10.1016/S0304-3835(98)00247-X)
14. Kim YS, Milner JA. Targets for indole-3-carbinol in cancer prevention. *J Nutr Biochem* 2005; 16:65-73; PMID:15681163; <http://dx.doi.org/10.1016/j.jnutbio.2004.10.007>
15. Ahmad A, Sakr WA, Rahman KM. Anticancer properties of indole compounds: mechanism of apoptosis induction and role in chemotherapy. *Curr Drug Targets* 2010; 11:652-66; PMID:20298156; <http://dx.doi.org/10.2174/138945010791170923>
16. Weng JR, Tsai CH, Kulp SK, Chen CS. Indole-3-carbinol as a chemopreventive and anti-cancer agent. *Cancer Lett* 2008; 262:153-63; PMID:18314259; <http://dx.doi.org/10.1016/j.canlet.2008.01.033>
17. Aggarwal BB, Ichikawa H. Molecular targets and anticancer potential of indole-3-carbinol and its derivatives. *Cell Cycle* 2005; 4:1201-15; PMID:16082211; <http://dx.doi.org/10.4161/cc.4.9.1993>
18. Malumbres M, Barbacid M. Cell cycle, CDKs and cancer: a changing paradigm. *Nat Rev Cancer* 2009; 9:153-66; PMID:19238148; <http://dx.doi.org/10.1038/nrc2602>
19. Lim S, Kaldis P. Cdk, cyclins and CKIs: roles beyond cell cycle regulation. *Development* 2013; 140:3079-93; PMID:23861057; <http://dx.doi.org/10.1242/dev.091744>
20. Weinberg RA. The retinoblastoma protein and cell cycle control. *Cell* 1995; 81:323-30; PMID:7736585; [http://dx.doi.org/10.1016/0092-8674\(95\)90385-2](http://dx.doi.org/10.1016/0092-8674(95)90385-2)
21. Chou TC, Talalay P. Quantitative analysis of dose-effect relationships: the combined effects of multiple drugs or enzyme inhibitors. *Adv Enzyme Regul* 1984; 22:27-55; PMID:6382953; [http://dx.doi.org/10.1016/0065-2571\(84\)90007-4](http://dx.doi.org/10.1016/0065-2571(84)90007-4)
22. Li P, Nijhawan D, Budihardjo I, Srinivasula SM, Ahmad M, Alnemri ES, Wang X. Cytochrome c and dATP-dependent formation of Apaf-1/caspase-9 complex initiates an apoptotic protease cascade. *Cell* 1997; 91:479-89; PMID:9390557; [http://dx.doi.org/10.1016/S0092-8674\(00\)80434-1](http://dx.doi.org/10.1016/S0092-8674(00)80434-1)
23. Fernandes-Alnemri T, Litwack G, Alnemri ES. CPP32, a novel human apoptotic protein with homology to *Caenorhabditis elegans* cell death protein Ced-3 and mammalian interleukin-1 beta-converting enzyme. *J Biol Chem* 1994; 269:30761-4; PMID:7983002
24. Rao XM, Zheng X, Waigel S, Zacharias W, McMasters KM, Zhou HS. Gene expression profiles of normal human lung cells affected by adenoviral E1B. *Virology* 2006; 350:418-28; PMID:16542696; <http://dx.doi.org/10.1016/j.virol.2006.02.009>
25. Zheng X, Rao XM, Gomez-Gutierrez JG, Hao H, McMasters KM, Zhou HS. Adenovirus E1B55K region is required to enhance cyclin E expression for efficient viral DNA replication. *J Virol* 2008; 82:3415-27; PMID:18234796; <http://dx.doi.org/10.1128/JVI.01708-07>
26. Cheng PH, Rao XM, Welcker M, McMasters KM, Zhou HS. Molecular basis for viral selective replication in cancer cells: activation of CDK2 by adenovirus-induced cyclin E. *PLoS One* 2013; 8:e57340; PMID:23437375; <http://dx.doi.org/10.1371/journal.pone.0057340>
27. Geng Y, Yu Q, Sicinska E, Das M, Schneider JE, Bhattacharya S, Rideout WM, Bronson RT, Gardner H, Sicinski P. Cyclin E ablation in the mouse. *Cell* 2003; 114:431-43; PMID:12941272; [http://dx.doi.org/10.1016/S0092-8674\(03\)00645-7](http://dx.doi.org/10.1016/S0092-8674(03)00645-7)
28. Geng Y, Lee YM, Welcker M, Swanger J, Zagodzko A, Winer JD, Roberts JM, Kaldis P, Clurman BE, Sicinski P. Kinase-independent function of cyclin E. *Mol Cell* 2007; 25:127-39; PMID:17218276; <http://dx.doi.org/10.1016/j.molcel.2006.11.029>
29. Ohtsubo M, Theodoras AM, Schumacher J, Roberts JM, Pagano M. Human cyclin E, a nuclear protein essential for the G1-to-S phase transition. *Mol Cell Biol* 1995; 15:2612-24; PMID:7739542
30. Le Cam L, Polanowska J, Fabrizzio E, Olivier M, Philips A, Ng Eaton E, Classon M, Geng Y, Sardet C. Timing of cyclin E gene expression depends on the regulated association of a bipartite repressor element with a novel E2F complex. *EMBO J* 1999; 18:1878-90; PMID:10202151; <http://dx.doi.org/10.1093/emboj/18.7.1878>
31. Ohtsubo M, Roberts JM. Cyclin-dependent regulation of G1 in mammalian fibroblasts. *Science* 1993; 259:1908-12; PMID:8384376; <http://dx.doi.org/10.1126/science.8384376>
32. Spruck CH, Won KA, Reed SI. Deregulated cyclin E induces chromosome instability. *Nature* 1999; 401:297-300; PMID:10499591; <http://dx.doi.org/10.1038/45836>
33. Minella AC, Welcker M, Clurman BE. Ras activity regulates cyclin E degradation by the Fbw7 pathway. *Proc Natl Acad Sci U S A* 2005; 102:9649-54; PMID:15980150; <http://dx.doi.org/10.1073/pnas.0503677102>
34. Ma Y, Fiering S, Black C, Liu X, Yuan Z, Memoli VA, Robbins DJ, Bentley HA, Tsongalis GJ, Demidenko E, et al. Transgenic cyclin E triggers dysplasia and multiple pulmonary adenocarcinomas. *Proc Natl Acad Sci U S A* 2007; 104:4089-94; PMID:17360482; <http://dx.doi.org/10.1073/pnas.0606537104>
35. Ries S, Korn WM. ONYX-015: mechanisms of action and clinical potential of a replication-selective adenovirus. *Br J Cancer* 2002; 86:5-11; PMID:11857003; <http://dx.doi.org/10.1038/sj.bjc.6600006>
36. Biederer C, Ries S, Brandts CH, McCormick F. Replication-selective viruses for cancer therapy. *J Mol Med (Berl)* 2002; 80:163-75; PMID:11894142; <http://dx.doi.org/10.1007/s00109-001-0295-1>
37. Chu RL, Post DE, Khuri FR, Van Meir EG. Use of replicating oncolytic adenoviruses in combination therapy for cancer. *Clin Cancer Res* 2004; 10:5299-312; PMID:15328165; <http://dx.doi.org/10.1158/1078-0432.CCR-0349-03>
38. Khuri FR, Nemunaitis J, Ganly I, Arsenau J, Tannock IF, Romel L, Gore M, Ironside J, MacDougall RH, Heise C, et al. A controlled trial of intratumoral ONYX-015, a selectively-replicating adenovirus, in combination with cisplatin and 5-fluorouracil in patients with recurrent head and neck cancer. *Nat Med* 2000; 6:879-85; PMID:10932224; <http://dx.doi.org/10.1038/78638>
39. Rodriguez-Rocha H, Gomez-Gutierrez JG, Garcia-Garcia A, Rao XM, Chen L, McMasters KM, Zhou HS. Adenoviruses induce autophagy to promote virus replication and oncolysis. *Virology* 2011; 416:9-15; PMID:21575980; <http://dx.doi.org/10.1016/j.virol.2011.04.017>
40. Reed GA, Peterson KS, Smith HJ, Gray JC, Sullivan DK, Mayo MS, Crowell JA, Hurwitz A. A phase I study of indole-3-carbinol in women: tolerability and effects. *Cancer Epidemiol Biomarkers Prev* 2005; 14:1953-60; PMID:16103443; <http://dx.doi.org/10.1158/1055-9965.EPI-05-0121>
41. Rao XM, Tseng MT, Zheng X, Dong Y, Jamshidi-Parsian A, Thompson TC, Brenner MK, McMasters KM, Zhou HS. E1A-induced apoptosis does not prevent replication of adenoviruses with deletion of E1b in majority of infected cancer cells. *Cancer Gene Ther* 2004; 11:585-93; PMID:15338010; <http://dx.doi.org/10.1038/sj.cgt.7700739>
42. Sandig V, Youil R, Bett AJ, Franklin LL, Oshima M, Maione D, Wang F, Metzker ML, Savino R, Caskey CT. Optimization of the helper-dependent adenovirus system for production and potency in vivo. *Proc Natl Acad Sci U S A* 2000; 97:1002-7; PMID:10655474; <http://dx.doi.org/10.1073/pnas.97.3.1002>
43. Zhao T, Rao XM, Xie X, Li L, Thompson TC, McMasters KM, Zhou HS. Adenovirus with insertion-mutated E1A selectively propagates in liver cancer cells and destroys tumors in vivo. *Cancer Res* 2003; 63:3073-8; PMID:12810631
44. Ishiyama M, Tomimaga H, Shiga M, Sasamoto K, Ohkura Y, Ueno K. A combined assay of cell viability and in vitro cytotoxicity with a highly water-soluble tetrazolium salt, neutral red and crystal violet. *Biol Pharm Bull* 1996; 19:1518-20; PMID:8951178; <http://dx.doi.org/10.1248/bpb.19.1518>
45. Kwon OJ, Kim PH, Huyn S, Wu L, Kim M, Yun CO. A hypoxia- and alpha-fetoprotein-dependent oncolytic adenovirus exhibits specific killing of hepatocellular carcinomas. *Clin Cancer Res* 2010; 16:6071-82; PMID:21169258; <http://dx.doi.org/10.1158/1078-0432.CCR-10-0664>